Plant Physiology Preview. Published on July 13, 2015, as DOI:10.1104/pp.15.01045

Running title: Metabolism supporting methacrolein absorption

All correspondence should be sent to:

Kenji Matsui

Department of Biological Chemistry, Faculty of Agriculture and the Department of Applied Molecular Bioscience, Graduate School of Medicine
Yamaguchi University, Yamaguchi 753-8515, Japan

Tel: +81-83-933-5850

E-mail: matsui@yamaguchi-u.ac.jp

Research area: Biochemistry and Metabolism

Glutathionylation and reduction of methacrolein in tomato plants account for its absorption from the vapor phase

Shoko Muramoto[1], Yayoi Matsubara[1], Cynthia Mugo Mwenda[1], Takao Koeduka[1], Takuya Sakami[2], Akira Tani[2], Kenji Matsui[1*]

[1]Department of Biological Chemistry, Faculty of Agriculture and Department of Applied Molecular Bioscience, Graduate School of Medicine
Yamaguchi University, Yamaguchi 753-8515, Japan

[2]Institute for Environmental Sciences, University of Shizuoka, Shizuoka 422-8526, Japan

Summary: Formation of adducts with glutathione and reduction facilitate the absorption of a reactive volatile chemical from the atmosphere in tomato plants.

Footnotes:

Financial source;
This work was supported partly by JSPS KAKENHI Grant Numbers 26660095 and 25282234, and the Yobimizu Project from Yamaguchi University.

*Corresponding author:
Kenji Matsui,
matsui@yamaguchi-u.ac.jp
Department of Biological Chemistry, Faculty of Agriculture and the Department of Applied Molecular Bioscience, Graduate School of Medicine, Yamaguchi University, Yamaguchi 753-8515, Japan. Tel: +81 (83) 933-5850; Fax: +81 (83) 933-5820;
E-mail: matsui@yamaguchi-u.ac.jp

Abstract

A large portion of the volatile organic compounds emitted by plants are oxygenated to yield reactive carbonyl species (RCSs), which have a big impact on atmospheric chemistry. Deposition to vegetation driven by the absorption of RCSs into plants plays a major role in cleansing the atmosphere, but the mechanisms supporting this absorption have been little examined. Here, we performed model experiments using methacrolein (MACR), one of major RCSs formed from isoprene, and tomato plants (*Solanum lycopersicum*). Tomato shoots enclosed in a jar with MACR-vapor efficiently absorbed MACR. The absorption efficiency was much higher than expected from the gas/liquid partition coefficient of MACR, indicating that MACR was likely metabolized in leaf tissues. Isobutyraldehyde, isobutyl alcohol, and methallyl alcohol (MAA) were detected in the headspace and inside tomato tissues treated with MACR-vapor, suggesting that MACR was enzymatically reduced. Glutathione (GSH) conjugates of MACR (MACR-GSH) and MAA (MAA-GSH) were also detected. MACR-GSH was essentially formed through spontaneous conjugation between endogenous GSH and exogenous MACR, and reduction of MACR-GSH to MAA-GSH was likely catalyzed by an NADPH-dependent enzyme in tomato leaves. Glutathionylation was the metabolic pathway most responsible for the absorption of MACR, but when the amount of MACR exceeded the available GSH, MACR that accumulated reduced photosynthetic capacity. In an experiment simulating the natural environment using gas flow, MACR-GSH and MAA-GSH accumulation accounted for 30-40% of the MACR supplied. These results suggest that MACR metabolism, especially spontaneous glutathionylation, is an essential factor supporting MACR absorption from the atmosphere by tomato plants. (248 words)

Introduction

Plants emit vast amounts of volatile organic chemicals (VOCs) into atmosphere. The annual emission of VOCs other than methane is estimated to be around 1300 Tg of carbon (Goldstein and Galbally, 2007), with approximately 90% originating from biogenic sources, of which one-third (ca. 500 Tg C/year) is isoprene (Guenther et al., 1995). In the atmosphere, VOCs undergo the chemical processes of photolysis and reaction with hydroxyl and nitrate radicals (Atkinson and Arey, 2003). Isoprene, for example, is converted into a series of isomeric hydroxyl-substituted alkyl peroxyl radicals, which are further converted into methyl vinyl ketone (but-3-en-2-one, MVK) and methacrolein (2-methylprop-2-enal, MACR) (Liu et al., 2013). These VOCs and their oxygenated products (oVOCs) are important components for the production of ozone and aerosols, and thus have a big impact on atmospheric chemistry and even on the climate system (Goldstein and Galbally, 2007). VOCs and oVOCs are removed from the atmosphere through oxidation to carbon monoxide or dioxide, dry or wet deposition, or secondary aerosol formation (Goldstein and Galbally, 2007). Among these, deposition to vegetation plays a major role in the removal of VOCs and oVOCs from the atmosphere (Karl et al., 2010).

A significant portion of the deposition to vegetation is attributable to the uptake of VOCs and oVOCs by plants, and a field study showed that MVK and MACR were immediately lost once they entered a leaf through stomata (Karl et al., 2010). Under growth conditions where stomatal conductance is high enough, the partitioning of VOCs between air and leaf water phases in equilibrium and the capacity of the plant to metabolize, translocate and store VOCs determine their uptake rate (Tani et al., 2013). The immediate loss in leaves observed with MVK and MACR is indicative of efficient enzymatic reactions metabolizing them; however, the details of the metabolism of these oVOCs have been little investigated so far.

The absorption and metabolism of several VOCs by plants have been reported. Airborne *ent*-kaurene was absorbed by *Arabidopsis thaliana*, *Chamaecyparis obtuse* (Japanese cypress), and *Cryptomeria japonica* (Japanese cedar) plants, and converted into gibberellins (Otsuka et al., 2004). *A. thaliana* absorbed (*Z*)-3-hexenal and converted it into (*Z*)-3-hexen-1-ol or further into (*Z*)-3-hexen-1-yl acetate, using NADPH and acetyl-CoA, probably inside the plant tissues (Matsui et al., 2012). *Nicotiana attenuata*

plants absorbed dimethyl disulfide formed by rhizobacteria (Meldau et al., 2013). The sulfur atom derived from volatile dimethyl disulfide was assimilated into plant proteins. Karl et al. (2010) assumed that aldehyde dehydrogenase, which is involved in detoxification that limits aldehyde accumulation and oxidative stress (Kirch et al., 2004), is involved in the uptake of oVOCs containing an aldehyde moiety; however, they did not provide direct evidence supporting their assumption.

Conjugation of VOCs and oVOCs with sugar or glutathione (GSH) is another way to metabolize them. (*Z*)-3-Hexen-1-ol in the vapor phase was taken up by tomato plants and converted into its glycoside (Sugimoto et al., 2014). (*E*)-2-Hexenal reacts with GSH spontaneously and/or via GSH transferase (GST) to form hexanal–GSH, which is subsequently reduced to hexanol–GSH (Davoine et al., 2006), although it is uncertain whether airborne (*E*)-2-hexenal is converted into its corresponding GSH-adduct. Glutathionylation of (*E*)-2-hexenal is common and has been confirmed in grapevine (*Vitis vinifera*) and passion fruit (*Passiflora edulis*) (Kobayashi et al., 2011, Fedrizzi et al., 2012). The catabolites formed from the GSH adduct in these crops are precursors for important flavor components.

Although it is clear that oVOCs are absorbed by vegetation and that their efficient uptake is probably supported by metabolism in plant tissues, the metabolic fates of oVOCs taken up from the vapor phase into plants have been little studied. Here, we performed a series of model experiments using tomato seedlings and MACR to dissect the fates of oVOCs once they entered into plant tissues. In order to clearly see absorption of MACR and its fates in plant tissues, a model experiment under enclosed condition with high concentration of MACR was first carried out. Subsequently, an airflow system with a realistically low concentration of MACR was employed. Tomato plants efficiently absorbed MACR. Reduction of the carbonyl moiety and the double bond conjugated to the carbonyl, and conjugation with GSH were the major metabolism of exogenous MACR. The metabolism seemed to be involved in the detoxification of reactive carbonyl species, which, in turn, accounted for the oVOC deposition to vegetation.

Results

Absorption of methacrolein in the headspace by tomato. To examine the absorption of methacrolein (MACR) by tomato plants, we placed the aboveground parts of 3- to 4-week-old tomato plants in a glass jar (187 mL), and a droplet (9.35 μL) of MACR solution [0.5 M dissolved in 3.5% (w/v) Tween 20] was absorbed into the tip of a cotton swab. The jar was tightly closed and placed under light at 25°C. Because the partial pressure of MACR in the jar (0.427 mm Hg) that would be expected if all the MACR was vaporized was lower than the vapor pressure of MACR (155 mm Hg) at 25°C, the MACR concentration would be 560 μL L^{-1}. A jar without a plant was used as a control. The headspace gas was sampled periodically, and the airborne carbonyl compounds in the headspace were quantified with HPLC after derivatization into their 2,4-dinitrophenylhydrazones. When the headspace was taken immediately (ca. 10 s) after the lid was closed, MACR was detected at its vapor concentration of 250 to 270 μL L^{-1} (Fig. 1A). Without a plant, the concentration in the headspace was 390 μL L^{-1} and remained mostly constant until 4 h. In the presence of a plant the headspace concentration of MACR dropped to 80 μL L^{-1} by 0.5 h. The concentration continued to decrease until 4 h. At 2 h, about 90% of the MACR was taken up by the tomato plant.

Reduction. In HPLC analysis of the headspace gas, we noticed the appearance of a peak corresponding to isobutyraldehyde (2-methylpropanal) that would be formed through reduction of the alkene moiety of MACR. At 0 h (10 s after the onset of the experiment), isobutyraldehyde was below the detection limit but at 0.5 h it increased to 30 μL L^{-1} (Fig. 1B). The amount of isobutyraldehyde detected at 0.5 h corresponded to 5.8% of the MACR used for the exposure. Its concentration in the headspace then decreased, and after 2 h it was almost undetectable. In the absence of the plant, no isobutyraldehyde formation was detected.

Previously, we showed that Arabidopsis plants absorbed (*Z*)-3-hexenal, reduced it into (*Z*)-3-hexen-1-ol, and thereafter, emitted (*Z*)-3-hexen-1-ol into the atmosphere (Matsui et al., 2012). Thus, we assumed that the reduction of aldehydes to alcohols would be one way of metabolizing airborne carbonyl compounds. To examine the reduction of the aldehyde moiety of MACR and re-emission of its reduced forms by tomato plants, the aerial part of tomato plant was exposed to 560 μL L^{-1} MACR-vapor

in a 187 mL-glass jar for 2 and 24 h, and VOCs in the headspace gas were extracted with dichloromethane and subjected to GC-MS analysis. Under the GC-MS conditions employed here, MACR and isobutyraldehyde could not be detected. No compound related to MACR was detected immediately after exposing tomato plants to MACR-vapor (Fig. 2A). At 2 h after exposure, 2-methylprop-2-en-1-ol (methallyl alcohol; MAA) and 2-methylpropan-1-ol (isobutyl alcohol) were detected only when MACR-vapor was incubated with tomato plants (Figs. 2A and S1). At 2 h, 0.96% and 1.6% of the MACR used for exposure was found as MAA and isobutyl alcohol in the headspace, respectively. At 24 h, their concentrations in the headspace decreased to less than 2 $\mu L\ L^{-1}$.

Because the reduction of carbonyls needs a reductant, such as NADH or NADPH, which are generally found inside cells, the reduction of MACR to MAA and isobutyl alcohol should proceed in the cells. Thus, we assumed that MAA and isobutyl alcohol were formed inside the tomato cells, and that a portion of each was emitted from the tissues to the headspace. Therefore, next, we extracted MACR metabolites from the leaves exposed to MACR-vapor at 560 $\mu L\ L^{-1}$ in a glass jar (187 mL) for 2 and 24 h. After extraction with dichloromethane, MAA formation in plant tissues was detected even after 3 to 4 s of MACR exposure (Fig. 2B). At that time, isobutyl alcohol was not detected in the plant tissues. Both MAA and isobutyl alcohol in the tissues increased at 2 h after exposure, and then decreased to low levels at 24 h. At 2 h, 6.5% and 5.6% of the MACR used for the exposure was detected as MAA and isobutyl alcohol in the tissues, respectively. Although we did not distinguish whether these alcohols really occurred in the plant tissue or were just attached to the plant surface, these alcohols should be formed from MACR taken up from the headspace into the tissues where a reductase-catalyzed reduction was operative (Matsui et al, 2012).

Glutathionylation. It has been reported that reactive carbonyl species harboring α,β-unsaturated carbonyl moieties are detoxified through conjugation with glutathione (GSH) (Davoine et al., 2005; Davoine et al., 2006; Mano, 2012). The conjugation reaction proceeds either spontaneously or enzymatically via GSH *S*-transferases (GST) (Davoine et al., 2006). Because MACR has the α,β-unsaturated carbonyl moiety, we assumed that a portion of the MACR taken up by tomato plants would be converted to its GSH adduct [*S*-3-(2-methylpropanal)glutathione, MACR-GSH] in the tissues. To

examine the formation of the conjugate, we first synthesized MACR-GSH, and established an analytical system with LC-MS/MS (Figs. S2 and S3).

When an extract prepared from tomato plants exposed to MACR-vapor at 560 μL L^{-1} in a glass jar (187 mL) for 2 h was subjected to LC-MS/MS analysis, we detected a peak corresponding to MACR–GSH. At the same time, a big peak with an *m/z* of 380 was detected. This peak coincided with the compound prepared from synthetic MACR–GSH through reduction with $NaBH_4$; thus, it was assigned as the GSH adduct of MAA [*S*-3-(2-methylpropan-1-ol)glutathione (MAA-GSH)]. The MS profiles of synthetic MAA-GSH and the compound detected in the MACR-exposed tomato tissues supported this assignment (Fig. S3). When the extract was analyzed in the neutral loss mode (−75 Da; corresponding to the removal of glycine) with the aim of detecting all GSH adducts, only peaks corresponding to MACR-GSH and MAA-GSH were detected (Fig. S4).

Next, we followed formation of MACR-GSH and MAA-GSH in tomato leaves exposed to 560 μL L^{-1} of MACR-vapor in a glass jar (187 mL) (Fig. 3). MACR-GSH and MAA-GSH were detected in tomato tissues even at 3 to 4 s after the onset of exposure . MACR-GSH was quickly formed, and at 1 min after exposure, the amount went up to 568 nmol g^{-1} FW (corresponding to 6.12% of the added MAC). The amount reached its maximum at 10 min, and thereafter gradually decreased. MAA-GSH, the reduced form of MACR-GSH, started to increase from 1 min after exposure, and reached its maximum level (1504 nmol g^{-1} FW, corresponding to 20.9% of the added MACR) at 30 min. The level was almost constant until 24 h.

GST activity to form MACR-GSH and reductase activity to form MAA-GSH.

To examine whether the formation of GSH adducts with MACR was catalyzed by GST or occurred spontaneously, we prepared a crude enzyme extract from tomato leaves and estimated the GST activity. When a common GST substrate, 1-chloro-2,4-dinitrobenzene, was used, no GST activity was detected. Spontaneous formation of MACR-GSH was detected just by mixing MACR and GSH in phosphate buffer at pH 6.5. The addition of crude enzyme solution into the reaction mixture hardly enhanced the reaction between MACR and GSH (Fig. S5). Thus, we failed to detect significant GST activity to form MACR-GSH in tomato leaves at least in vitro.

MAA-GSH should be formed from MACR-GSH through reduction of the

carbonyl group originating from MACR. Reduction of the aldehyde group in the GSH-adduct derived from (*Z*)-3-hexenal was supposed in tobacco leaves and grapevine based on the metabolites found in these plant tissues (Davoine et al., 2006, Kobayashi et al., 2011). When MACR-GSH was incubated with crude enzyme solution in the presence of NADPH, MAA-GSH formation was detected (Fig. 4). The addition of NADH also enhanced MACR-GSH reduction, but to a lesser extent than NADPH. Heat-denatured enzyme solution failed to enhance the reduction even in the presence of NADPH. The MACR-GSH to MAA-GSH reduction activity was inducible, and higher activity was detected in tomato leaves exposed to MACR-vapor at 560 μL L^{-1} in a glass jar (187 mL) for 2 h (Fig. 4).

MACR absorption in a flow system. The experimental system employed in this study to expose tomato plants to MACR-vapor in an enclosed jar helped us clarify the metabolism of MACR as shown above; however, in a natural environment, plants are exposed to VOCs in airflow. The concentration of MACR in natural environments ranges from sub- to several nL L^{-1} levels (Jardine et al., 2012; Jardine et al., 2013; Kalogridis et al., 2014). To confirm whether the MACR metabolism in tomato plants observed in the enclosed experimental system also operated in an airflow system with a realistically low concentration of MACR, we set up an airflow system to expose tomato plants (Tani et al., 2013). Because glutathionylation was the main metabolism of MACR according to the results with the enclosed exposure system and the sensitivity of GSH adduct detection in the LC-MS/MS system used in this study was high, we focused on glutathionylation. In our airflow system, tomato plants grown in pots were exposed to airflow containing 0, 20, or 100 nL L^{-1} MACR at 1.5 L min^{-1} in a transparent, fluorinated ethylene-propylene copolymer bag (20 to 40 L) for 6 h under illumination. We set the MACR concentration of 100 nL L^{-1} as well in order to estimate the capacity of tomato plants to absorb and metabolize MACR. After exposure, leaves were harvested for LC-MS/MS analysis of the GSH adducts.

During the exposure to the flow of clean air, tomato plants emitted isoprene and MACR at the rates of 8.90 ± 3.58, and 4.67 ± 1.08 fmol g^{-1} FW s^{-1}, respectively. Net photosynthetic rate was largely constant at 21.2 ± 1.50 nmol (CO_2) s^{-1} $plant^{-1}$, and transpiration rate was 2.44 ± 0.06 μmol (H_2O) s^{-1} $plant^{-1}$. Tomato plants exposed to clean air for 6 h had trace amounts of MACR-GSH and MAA-GSH (Table I). After

273 exposure to 20 nL L^{-1} MACR, accumulation of 1.47 ± 0.14 and 37.9 ± 2.84 nmol g^{-1}
274 FW of MACR-GSH and MAA-GSH, respectively, was detected. With 100 nL L^{-1} of
275 MACR, the amounts of MACR-GSH and MAA-GSH went up to 6.51 ± 0.87 and 153 ±
276 15.7 nmol g^{-1} FW. Even after exposure to 100 nL L^{-1} MACR for 6 h, no visible
277 symptoms of MACR toxicity were detected. Because we exposed five tomato plants of
278 ca. 1 g FW in each bag, the total amounts of GSH adducts in the tomatoes in the bag
279 were estimated to be 197 and 798 nmol, respectively, at 20 and 100 nL L^{-1} MACR. This
280 suggested that as much as ca. 41% and 33% of the airborne MACR supplied in airflow
281 (0.48 and 2.41 μmol, respectively) was absorbed by the tomato plants and converted
282 into GSH adducts.
283
284 **The capacity of MACR metabolism is limited.** To estimate the capacity of tomato
285 plants to absorb and metabolize MACR, the plants were exposed to 0, 112, 560, or 2240
286 μL L^{-1} MACR in an enclosed glass jar (187 mL) for 2 h, and the MACR left in the
287 headspace was quantified (Fig. 5A). The tomato plants absorbed almost all MACR in
288 the headspace at a concentration of 112 μL L^{-1}. At this concentration, almost all MACR
289 absorbed by the tomato was converted into GSH adducts (Fig. 5C). The total GSH level
290 (GSH plus GSSG) was significantly lowered after 2 h exposure to MACR at 112 μL L^{-1}
291 (Fig. 5D). Isobutyraldehyde formation was not detected in this treatment (Fig. 5B). With
292 560 μL L^{-1} of MACR in the vapor phase, ca. 12% of the MACR (corresponding to 69.4
293 μL L^{-1}) was left in the headspace. At this concentration, the amounts of GSH adducts
294 barely increased from the values found with 112 μL L^{-1} MACR treatment, while the
295 total GSH level was lowered to ca. 10% of that found in control leaves.
296 Isobutyraldehyde was emitted from the plants, but accounted for only 7% of the MACR
297 used for the exposure. The amounts of GSH adducts were still almost the same even
298 when the plants were exposed to 2240 μL L^{-1}. The amount of isobutyraldehyde
299 accounted for 6.5%. Because of the limits of MACR metabolism, a large amount (ca.
300 54.3%) of the MACR used for exposure remained after 2 h.
301 Reactive carbonyl species are deleterious to plants at high concentrations
302 (Farmer and Mueller, 2013, Matsui et al., 2012, Mano, 2012). This is because the
303 capacity of plants to detoxify reactive carbonyl species is limited, and surplus chemicals
304 react with biological molecules inside plant tissues. The deleterious effect of MACR
305 that was not detoxified (leftover) in tomato tissue was estimated by measuring the

306 *Fv/Fm* ratio, as an indicator of stress on photosynthetic machinery (Baker & Rosenqvist,
307 2008), after exposing tomato plants to different concentrations of MACR-vapor for 2 h.
308 The *Fv/Fm* values was not affected when tomato plants were exposed to MACR-vapor
309 at 112 μL L^{-1}, but the value was lowered when the plants were exposed to higher
310 concentrations, such as 560 and 2240 μL L^{-1} (Fig. 5E). The degree of damage caused by
311 MACR correlated with the amount of MACR left in the jar after 2 h. After exposing the
312 plants to MACR for 2 h, they were taken out of the jar and incubated for an additional
313 19 h under the same light and temperature conditions but without MACR. The
314 pretreatment with MACR at 2240 μL L^{-1} for 2 h resulted in withering of leaves after 19
315 h, while the *Fv/Fm* values with plants pretreated with 560 μL L^{-1} after 19 h-recovery
316 were not different from those pretreated without or with low (112 μL L^{-1}) concentration
317 of MACR-vapor (Fig. S6).
318
319
320

Discussion

We showed that tomato shoots efficiently absorb MACR in the vapor phase under the experimental conditions employed here. The vapor pressure of MACR is 155 mm Hg at 25°C (PubChem, http://www.ncbi.nlm.nih.gov/pccompound); thus, 4.7 μmol of MACR in a 187 mL jar should be mostly in the vapor phase. Henry's law coefficient for MACR is 6.5 ± 0.7 mol L^{-1} atm^{-1} (Iraci et al., 1999). Under equilibrium conditions obeying the ideal gas law, $R_{aq/g} = HLRT$, where $R_{aq/g}$ is the ratio of the compound in aqueous phase to gas phase, H is the Henry's law coefficient (mol L^{-1} atm^{-1}), L is the liquid content [cm^3 cm^{-3}; ca 0.8 cm^3 water content (ca. 80% water content in ca. 1.0 g FW of tomato placed in the jar) in a 187 cm^3 jar (corresponding to 4.28×10^{-3}), R is the ideal gas constant (0.08206 L atm K^{-1} mol^{-1}), and T is the absolute temperature (298 K) (Iraci et al., 1999). Under our experimental conditions, $R_{aq/g}$ was calculated as 0.68; thus, the amount of MACR in the water phase (in tomato tissues) was estimated to be 1.89 μmol while 2.81 μmol of MACR still remained in the vapor phase under equilibrium. The results in this study clearly showed that MACR in the gas phase almost completely disappeared in the presence of tomato shoots. This indicates that MACR is metabolized inside the plant. Metabolite analyses showed that reduction of the double bond conjugated to the carbonyl, reduction of the aldehyde moiety, and glutathionylation played major roles in the metabolism of MACR to support its active uptake (Fig. 6).

Reduction of the double bond conjugated to a carbonyl moiety is one of pathways for detoxifying cytotoxic reactive carbonyl species harboring an α,β-unsaturated carbonyl moiety (Mano, 2012). In cucumber and Arabidopsis, NADPH-dependent alkenal/one oxidoreductases (AORs) are involved in the reduction of the double bond (Yamauchi et al., 2011). Another pathway for detoxification of reactive carbonyl species reduces the carbonyl to alcohol, and is catalyzed by aldo-keto reductases (AKRs) that also prefer NADPH as the reducing cofactor (Yamauchi et al., 2011, Matsui et al., 2012). The analysis of metabolites in tomato exposed to MACR-vapor indicated that both AORs and AKRs were involved in metabolizing MACR in tomato tissues. Because AORs require an α,β-unsaturated carbonyl moiety, isobutyl alcohol should be formed through AOR-dependent reduction of the double bond of MACR to yield isobutyraldehyde, followed by AKR-dependent reduction of isobutyraldehyde to yield isobutyl alcohol. A portion of this isobutyraldehyde was

354 released from the tissue, and a substantial amount of isobutyraldehyde was detected in
355 the jar after 2 h. However, the isobutyraldehyde in the jar almost completely
356 disappeared thereafter, which implies that the tomato plant re-absorbed
357 isobutyraldehyde, dependent on a metabolism to further reduce it to isobutyl alcohol.
358 This observation does not exclude the possibility that a portion of these metabolites is
359 derived from endogenous sources. We found that tomato emitted MACR at the rate of
360 0.38 ± 0.09 nL g^{-1} FW h^{-1}. Therefore, low but substantial contribution (up to 0.1%) of
361 MACR produced by plants should also be considered.

362 Because the reducing equivalents, i.e., NADH and NADPH, are essential to
363 both reductases and their contents in plant tissues are generally less than 10 nmol g^{-1}
364 FW (Guillaume and Noctor, 2007), regeneration of these cofactors would be necessary
365 to support the reduction to form 40 (MAA in headspace) to 360 (MAA in tomato tissue)
366 nmol g^{-1} FW of the reduced products (Fig. 2). This could be achieved only through
367 continuous regeneration of NADPH and NADH from $NADP^+$ and NAD^+ via the active
368 primary metabolism in intact cells. This indicates that the reduction is accomplished
369 inside the cells and that it is an active process requiring substantial resources that could
370 otherwise be used for plant growth.

371 The genes for AOR and AKR form a family, and each member shows distinct
372 substrate specificity (Yamauchi et al., 2011, Saito et al., 2013). As far as we know, an
373 enzyme with high specificity for MACR has not been reported so far; therefore, we do
374 not know if there is a reductase specific to MACR. Identification of the reductase(s)
375 involved in the reduction of MACR to MAA and isobutyl alcohol should be carried out.
376 Because we observed reduction to MAA in tomato tissue even within several seconds
377 after the onset of exposure (Fig. 2B), there should be substantial activity in tomato
378 shoots even before MACR exposure.

379 Based on the amounts of metabolites formed from MACR, conjugation of
380 MACR with GSH was assumed to be an important mechanism accounting for the
381 uptake of MACR by tomato plants. MACR-GSH was formed spontaneously at pH 6.5
382 just by mixing MACR and GSH, and we could not detect GST activity in tomato leaves
383 to enhance this spontaneous formation. Therefore, we assume that spontaneous
384 conjugation between MACR and GSH largely accounts for the formation of
385 MACR-GSH in tomato leaves exposed to MACR-vapor, and enzymatic formation via
386 GST has little if any contribution. The second-order rate constant of MACR and GSH in

387 phosphate buffer (pH 6.8) is as high as 203 L mol^{-1} min^{-1} (Böhme et al., 2010). This
388 high reaction rate explains the quick formation of MACR-GSH adduct well, even
389 without GST.

390 The amount of GSH in the tomato seedlings used in this study was estimated
391 to be 0.2 μmol g^{-1} FW (cf. Fig. 5D). When a tomato shoot (ca. 1 g FW) was exposed to
392 112 μL L^{-1} MACR in a 187 mL jar (0.94 μmol of MACR), more than 1 μmol g^{-1} FW of
393 GSH adducts (the sum of MACR-GSH and MAA-GSH) was formed (Fig. 5C).
394 Therefore, de novo replenishment of GSH would be essential for the formation of this
395 amount of GSH-adducts. Transgenic tomatoes having lower γ-glutamylcysteine
396 synthetase and/or glutathione synthetase activities showed lower capacity to decompose
397 chlorothalonil, a fungicide (Yu et al., 2013). The genes for γ-glutamylcysteine
398 synthetase and glutathione synthetase were induced when Arabidopsis was exposed to
399 ozone (Yoshida et al., 2009). Taken together, a system to replenish GSH is one of the
400 keys to meeting the demand brought about under stressed conditions.

401 MACR-GSH was further reduced to form MAA-GSH by a reductase in a
402 NADPH dependent manner. The MACR-GSH to MAA-GSH reduction activity was
403 induced after exposing plants to MACR, which implies that the enzyme responsible for
404 this reduction is involved in plant responses to the stress caused by MACR exposure. In
405 *Nicotiana tabacum*, GSH-adducts with keto fatty acids and 12-oxophytodienoic acid
406 were found with the ketone group; conversely, in *N. tabacum* and *V. vinifera*, a
407 GSH-adduct formed from (*E*)-2-hexenal was found as its reduced form (i.e.,
408 *S*-3-(hexan-1-ol)-glutathione) (Davoine et al., 2005; 2006; Kobayashi et al., 2011). Thus,
409 it was suggested that the reductase acting on GSH adducts preferred aldehydes to
410 ketones. MAA-GSH persisted for at least 6 h, but its amount was slightly decreased at
411 24 h. Degradation of the GSH-adduct catalyzed by γ-glutamyl transferase, such as that
412 found in grapevine (Kobayashi et al., 2011), might be involved in the degradation of
413 MAA-GSH.

414 At a lower concentration of MACR (112 μL L^{-1} in a 187 mL jar), almost all
415 of the MACR was absorbed by the tomato plant and metabolized essentially into its
416 GSH adducts (Fig. 5). Therefore, the tomato suffered little deleterious effect on its
417 photosynthetic apparatus at this low concentration of MACR even though the total GSH
418 levels were lowered to 60% of the control. Because of the efficient removal of MACR
419 through glutathionylation at a low concentration, the reduction to form isobutyraldehyde

was not functioning. At higher MACR concentrations, such as 560 and 2240 μL L^{-1}, the amount of GSH adducts formed in the tissue was almost the same as in the plant exposed to 112 μL L^{-1} MACR. This should essentially be because of limited GSH availability in the tomato tissue. The replenishment of GSH probably fell short, and as a result, the GSH pool was almost empty shortly after the plant was exposed to MACR at 560 and 2240 μL L^{-1}. Reduction of MACR became apparent at high concentrations, which would partly account for its detoxification. However, the ability to reduce MACR was insufficient at high concentrations, and some of the MACR partitioned into tissues would remain as MACR. The substantial concentrations of MACR in the vapor phase after 2 h exposure at 560 and 2240 μL L^{-1} clearly suggested that a substantial amount of MACR stayed in the tissues according to Henry's law. At 2 h after exposing tomato shoots to 2240 μL L^{-1} MACR in a closed jar, 1331 μL L^{-1} MACR still remained in the vapor phase, and under these conditions, it was assumed that the MACR concentration in the tissue might go up to 7.55 μmol g FW^{-1}. The 'leftover' from MACR metabolism had a deleterious effect on plant cells as evidenced by the suppression of PSII activity with MAC-exposure at 560 and 2240 μL L^{-1}.

These lines of evidence indicated that MACR uptake was largely supported by MACR metabolism inside the tomato tissue and that spontaneous reaction of MACR with GSH was most responsible for its metabolism, especially when the MACR concentration was less than 112 μL L^{-1}. The reduction of MACR might support its metabolism, especially at higher concentrations. Thus, the amount of GSH in the tissue is one of the keys to the cleansing of oVOCs from the atmosphere by vegetation. Many other reactions of oVOCs, such as oligomer formation (Liu et al., 2012) or reaction with hydrogen peroxide (Schöne and Herrmann, 2014), are still possible. Their contribution to the cleansing of oVOCs by vegetation should also be evaluated in future studies.

There are many chemical species of oVOCs in the atmosphere, and the absorption rates determined for them under realistic conditions using flow systems vary widely. Tani and Hewitt reported that plants absorbed aldehydes more efficiently than the corresponding ketones (Tani and Hewitt, 2009). Acetone, for example, was only partly taken up by plants at the beginning of exposure because of the partition into plant tissues, but not continuously taken up, probably because no metabolism is expected for this ketone. The situation is also the same with *Populus nigra* and *Camellia sasanqua*. In these species, acrolein and methyl ethyl ketone were taken up efficiently, but acetone,

acetonitrile, isobutyl methyl ketone, chloroform, and benzene were essentially not taken up (Omasa et al., 2000). These observations also support that metabolism inside plant tissues is indispensable for cleansing oVOCs from the atmosphere. In our experimental system, at a reasonably low MACR concentration with a flow system simulating the natural environment, glutathionylation proceeded quite efficiently, and as much as 30% to 40% of the MACR flowing over tomato plants was absorbed and converted into its adducts. This implies that glutathionylation is one of the major metabolic pathways supporting the active absorption of oVOCs by tomato plants.

Harnessing the high ability of plants to metabolize oVOCs would be one way to manage air pollutants. To cope with the accumulation of anthropogenic as well as biogenic oVOCs, first we need to know the metabolic pathways responsible for their uptake by vegetation. We should investigate whether glutathionylation and reduction reactions are intrinsic to the cleansing of oVOCs in the other plant species. Also, continuous monitoring of GSH adducts formed from some oVOCs in the field would give insight into the contribution of glutathionylation to the deposition of oVOCs to vegetation.

Materials and Methods

Plants materials and growth conditions. Seeds of wild type tomato plants (*Solanum lycopersicum* cv. Micro-tom) obtained from the Agriculture and Forestry Research Center (Chiba, Japan) were grown under 14 h light (fluorescent lights at 60 μmol m^{-2} s^{-1})/10 h dark conditions at 25°C on soil composed of vermiculite and Takii Tanemakibaido (Takii and Co. Ltd., Kyoto, Japan) (volume ratio of 1:1) in a plastic pot (6-cm i.d.). The tomato plants were watered every 3 d with Hyponex Concentrated Liquid (HYPONeX JAPAN Co. Ltd., Osaka, Japan) diluted to 0.1%.

MACR-vapor treatment on tomato plants. The aerial parts of 3- to 4-week-old tomato were cut at the stem-root junction. The cut surface was covered with water-soaked cotton and then aluminum foil. The shoot was exposed to MACR (Sigma-Aldrich Co., St. Louis, MO, USA)-vapor in a 187-mL glass jar. For the treatment, 9.35 μL of MACR dissolved in 3.5% (w v^{-1}) Tween 20 at 0.5 M was

impregnated in a cotton swab, and the swab was attached to the aluminum cap of the jar. The concentration of MACR in the inner space of jar would be 560 μL L^{-1}. For treatment at lower concentrations, the MACR solution was sequentially diluted with 3.5% (w v^{-1}) Tween 20 (e.g., 0.1 M for 112 μL L^{-1}, or 0.02 M for 22.4 μL L^{-1}) and 9.35 μL of it was impregnated in the cotton swab. For 2240 μL L^{-1}, 131 μg of neat MACR was directly impregnated in the cotton swab. The jar was placed in a chamber under the same conditions used to grow the tomato plants. Control plants were exposed to water vapor. A jar without a plant was also prepared as a control to see the spontaneous degradation of MACR under the experimental conditions employed here. To measure the *Fv/Fm* values of the tomato, we used intact tomato plants without cutting the aerial part from pots in order to follow recovery from damage caused by MAC-exposure at 19 h after the treatment. Three tomato plants grown in soil in pots were exposed to MACR-vapor in a 3-L glass jar, and incubated under the same conditions as described above.

To expose tomato plants to airflow containing vaporized MACR, we enclosed five tomato plants grown in soil in pots in a transparent, fluorinated ethylene-propylene copolymer (FEP) bag (20 to 40 L). The open side of the bag was closed with a cable tie, and air was introduced into the bag via an inlet port at a flow rate of 1.5 L min^{-1}. VOCs and other contaminants including ozone from the inflow air were removed with a platinum catalysis heated to 400°C. The plants were illuminated with a 400 W metal halide lamp (D400, Toshiba LiTec, Tokyo, Japan). The photosynthetic photon flux density was held at 100 μmol m^{-2} s^{-1} at the top of the plants. The temperature in the bag was measured with T-type fine-wire thermocouples and set at 25 to 27°C during the exposure (for 6 h). Water vapor concentrations and the carbon dioxide concentrations of the inlet and outlet air were measured with CO_2/H_2O gas analyzer (LI-840A, LI-COR, Lincoln, NE). A constant concentration of MACR-vapor was maintained with a gas generator (PD-1B, Gastec, Kanagawa, Japan), and adjusted to 20 or 100 nL L^{-1} by mixing the MAC-containing air with clean air generated by blowing room air through Pt catalyst heated to 400°C at a given ratio. After exposure, the leaves were harvested and snap-frozen with liquid nitrogen for further analysis. In order to quantify the amounts of isoprene and MACR emitted from tomatoes, tomato plants in pots were placed in the bag of airflow system as above, and a portion of the outlet air was introduced through an adsorbent tube containing 200 mg Tenax-TA and 100 mg

519 Carbotrap at a flow rate of 200 mL min^{-1} for 20 min by using a portable pump
520 (MP-Sigma30, Shibata Inc., Tokyo, Japan). The collected samples were identified and
521 quantified with a GC-MS (QP5050A, Shimadzu, Kyoto, Japan) equipped with a thermal
522 desorption system (Turbo matrix ATD, Perkin Elmer Instruments, Waltham, MA).
523 Compound separation was achieved using an SPB-5 capillary column (50 m x 25 mm, 1
524 mm film thickness) (Mochizuki et al., 2014).
525
526 **Measurement of the *Fv/Fm* ratio.** The *Fv/Fm* ratio, as a parameter relating the
527 maximum quantum yield of photosystem II (PSII), was estimated from chlorophyll
528 fluorescence measurements using a pulse amplitude modulated (PAM) fluorometer
529 (Mini-PAM photosynthesis yield analyzer; Walz, Effeltrich, Germany). The saturation
530 pulse duration was 0.8 s with an intensity level of approximately 8300 μmol m^{-2} s^{-1}.
531 After exposure to MACR-vapor, the tomato plants were placed in the dark for 30 min,
532 and then fluorescence measurements were conducted at the center of the leaves.
533
534 **Measurement of MACR in the headspace of the glass jar.** A tomato plant was
535 exposed to 560 μL L^{-1} (in vapor) MACR in a glass jar. After closing the cap, the
536 headspace air (10 mL) in the jar was collected with a gas-tight syringe through a silicon
537 rubber septum (6 mm i.d.) inserted into a hole made at the center of the lid. The air was
538 introduced into a closed glass vial containing a mixture of acetonitrile (400 μL), 20 mM
539 2,4-dinitrophenylhydrazine (2,4-DNPH) (100 μL), formic acid (20 μL), and 10 mM
540 2-ethylhexanal [internal standard (IS), 10 μL] (Alfa Aesar, Lancashire, United
541 Kingdom). The mixture was vigorously vortexed for 2 min and left for 30 min under
542 dark conditions at room temperature. After incubation, the mixture was transferred to a
543 glass tube containing 1 mL of water and 2 mL of ethyl acetate, mixed vigorously, and
544 centrifuged at 1000 *g* for 10 min. The organic layer was collected and subjected to
545 HPLC analysis. The hydrazone derivatives were analyzed using a HPLC system with a
546 Mightysil RP-18 GP column (Kanto Chemical Co., Tokyo, Japan) as described by
547 Matsui et al. (2009). For the quantification of each compound, calibration curves were
548 constructed using IS and standard compounds, MACR and isobutyraldehyde (Wako
549 Pure Chemical Industries, Ltd., Osaka, Japan).
550
551 **Analysis of the metabolites derived from MACR in the headspace and tomato**

552 **tissues.** The air (10 mL) in the jar taken with a gas-tight syringe was introduced into a
553 tightly closed glass vial containing 1 mL of CH_2Cl_2 with 50 ng mL^{-1} nonyl acetate
554 (Tokyo Chemical Industry Co., Tokyo, Japan) as an IS. The vial was vigorously
555 vortexed for 2 min, and the solution was subsequently concentrated with N_2 gas to ca.
556 100 μL for GC-MS analysis using a GC-MS (QP-5050, Shimadzu, Kyoto, Japan)
557 equipped with a DB-Wax column (30-m length × 0.25-mm i.d. × 0.25-μm film
558 thickness, Agilent Technologies, Santa Clara, CA, USA). The column temperature was
559 programmed as follows: 40°C for 5 min, increasing by 10°C min^{-1} to 200°C for 5 min.
560 The carrier gas (He) was delivered at 86.1 kPa. The sample size was 1 μL and the split
561 ratio was 2. The temperatures of the injector and interface were 240 and 200°C,
562 respectively. The mass detector was operated in the electron impact mode with
563 ionization energy of 70 eV. Identification of the alcohols was performed by comparing
564 their retention times and mass spectra with those of standard compounds, MAA (Tokyo
565 Chemical Industry Co.) and isobutyl alcohol (Sigma-Aldrich Co.). The amount of each
566 compound was calculated with a calibration curve based on the area ratio of the sample
567 to the IS.
568 To analyze the metabolites derived from MACR in tomato leaves, the leaves
569 were wrapped in aluminum foil and snap-frozen in liquid nitrogen. The frozen leaves
570 wrapped in foil were crushed with a hammer to make leaf powder in liquid nitrogen.
571 The powder was placed in a plastic tube with 8 stainless beads (3 mm in diameter) at
572 −80°C until extraction. The stored samples were further crushed with a beads cell
573 disruptor (Micro Smash MS100R; TOMY Digital Biology, Co., Tokyo, Japan) for 1 min
574 at 3500 rpm, keeping the materials frozen. To the leaf powder (100 mg) of tomato, 1 mL
575 of CH_2Cl_2 containing 500 ng mL^{-1} nonyl acetate as an IS was added and homogenized
576 for 1 min at 3500 rpm with the beads cell disruptor. The sample was centrifuged for 10
577 min at 12,000 × *g* with the T16A31 rotor (Hitachi Koki, Co., Tokyo, Japan). The
578 CH_2Cl_2 layer was transferred into a new glass tube. After concentration with N_2 gas to
579 100 μL, the compounds in solution were analyzed by GC-MS as described above. The
580 amounts of alcohols were calculated with the corresponding calibration curves
581 constructed with authentic compounds based on the area ratio to the IS.
582
583 **Synthesis of GSH conjugates.** To obtain MACR-GSH with high purity, 3.25 mmol of
584 GSH (Wako Pure Chemical Industries, Ltd.) was mixed with an excess amount (24.2

585 mmol) of MACR in 20 mM borate buffer, pH 10.0 and reacted for 1 h under an argon
586 atmosphere. The reaction was stopped by adjusting the pH to 4.0 with 10% formic acid,
587 and the surplus MACR was evaporated out with N_2 gas flow. Complete consumption of
588 GSH was confirmed by TLC analysis on silica plates (Silica gel 60 F254, Merck KGaA,
589 Darmstadt, Germany) using acetonitrile/water/acetic acid (80/20/0.1, v/v) as the
590 developing solvent. The compounds were visualized with anisaldehyde or ninhydrin
591 reagent. The product was freeze-dried and subjected to LC-MS/MS analysis. A total ion
592 chromatogram obtained with the enhanced mass (EMS) mode indicated >90% purity of
593 MACR-GSH. MAA-GSH was synthesized by adding an excess amount of $NaBH_4$ to
594 MACR-GSH in 20 mM borate buffer, pH 10.0. Identification of the compounds was
595 performed by LC-MS/MS with EMS mode (Fig. S4) using a LC-MS/MS [3200
596 Q-TRAP LC/MS/MS System (AB Sciex, Framingham, MA, USA) equipped with a
597 Prominence UFLC (Shimadzu, Kyoto, Japan)]. The products were separated on a
598 Mightysil RP18 column (150-mm × 2-mm i.d.) with a binary gradient consisting of
599 water:formic acid (100:0.1, v/v, solvent A) and acetonitrile:formic acid (100:0.1, v/v,
600 solvent B). The run consisted of 100% A for 5 min, a linear increase from 100% A to
601 100% B over 25 min (flow rate, 0.2 mL min^{-1}), and 100% B for 2 min. Compounds
602 were detected by MS/MS using electro-spray ionization in the positive ion mode [ion
603 spray voltage: 5000 V, nitrogen as both the curtain gas (set to 20 arbitrary units) and
604 collision gas (set to 'high'), collision energy: 19 V, scan range: *m/z* 100 to 1200, scan
605 speed: 4,000 Da s^{-1}, declustering potential: 26 V].
606
607 **Analysis of GSH adducts in tomato leaves**. The frozen powder prepared from tomato
608 leaves (80 mg) was suspended in 1 mL of 20 mM borate buffer, pH 4.0 containing 5 µg
609 of *S*-hexylglutathione (Hex-GSH) (Sigma-Aldrich Co.) as an IS. The GSH-adducts were
610 extracted with a beads cell disruptor for 1 min at 3500 rpm. The suspension was
611 centrifuged at 8000 *g* for 15 min at 4°C. The supernatant was filtered through an
612 Ekicrodisc 3 (HPLC Certified, 0.45 µm, 3 mm; Pall Corporation, Port Washington, NY).
613 GSH conjugates in the extract were scanned by analysis in the EMS mode as shown
614 above or in the neutral loss mode, which permitted the determination of the *m/z* ratio of
615 pseudomolecular ions undergoing neutral loss of 75 mass units (part of glycine) upon
616 fragmentation of the compounds under the same MS conditions used in EMS mode. The
617 compounds were identified by comparing the mass spectra (obtained with EMS mode)

618 and their retention times with those of standard compounds. For quantification of GSH
619 conjugates in the sample, LC-MS/MS analysis in the multiple reaction monitoring
620 (MRM) mode was performed. A calibration curve was constructed with the synthesized
621 MACR-GSH and MAA-GSH based on their area ratio to hex-GSH. The parameters
622 used for MRM detection are shown in Table S1. Total GSH (GSH + GSSG) was
623 determined with the enzymatic recycling assay based on glutathione reductase and
624 5,5′-dithiobis-(2-nitrobenzoic acid) as described by Griffith (1980).
625
626 **GST and reductase assay**. The crude enzyme solution for GST and reductase assay
627 was prepared according to a procedure described previously (Davoine et al, 2006).
628 Tomato leaves (0.5 to 0.7 g FW) were homogenized with 50 mM potassium phosphate
629 buffer (pH 7.2) containing 2 mM dithiothreitol, 0.01% Triton X-100, 1 mM EDTA, and
630 8% polyclar VT using a mortar and pestle. After filtration with cheesecloth, the sample
631 was centrifuged at 14,500 *g* at 4°C for 20 min. The supernatant was used for the assay.
632 The protein content was determined using a Bio-Rad Protein Assay (Bio-Rad
633 Laboratories, Inc., Hercules, CA, USA).
634 For GST activity assay, the absorption at 340 nm was monitored with a
635 reaction solution (1 mL) containing 1 mM 1-chloro-2,4-dinitrobenzene (CDNB), 1.5
636 mM GSH, and crude enzyme solution (100 μL) in 50 mM potassium phosphate buffer,
637 pH 7.2 at 25°C for 3 min. To estimate the GST activity to form MACR-GSH, a reaction
638 solution (0.5 mL) containing 0.2 mM MACR, 0.3 mM GSH, and crude enzyme solution
639 (10 μL) in 100 mM potassium phosphate buffer, pH 7.2 was prepared and reacted for 1
640 and 10 min. The reaction was stopped by adjusting the pH to 4.0 using 10% (v/v)
641 formic acid. The mixture was filtered and subjected to LC-MS/MS analysis to quantify
642 the MACR-GSH. Control reactions were done without enzyme solution and with
643 heat-denatured (100°C for 10 min) enzyme solution.
644 The enzymatic activity to reduce MACRS-GSH to MAA-GSH was examined
645 by monitoring the product with LC-MS/MS. A reaction mixture (500 μL) containing 0.2
646 mM MACR-GSH, 4 mM NADH or NADPH, and crude enzyme solution (10 μL) in 50
647 mM potassium phosphate buffer, pH 7.2 was reacted for 10 min. After incubation, the
648 reaction was stopped by adjusting the pH to 4.0. The GSH adducts formed through
649 enzymatic reaction were quantified by LC-MS/MS analysis in MRM mode.
650

Statistics. Statistical analyses were conducted using "Excel toukei" (Social Survey Research Information Co. Tokyo, Japan). When two factors were considered, we used two-way ANOVA followed by Tukey's post hoc test, whereas for single factors one-way ANOVA followed by Tukey's post hoc test was applied. The accumulation of GSH adduct in the airflow experiment was evaluated with a *t*-test.

Figure legends

Figure 1. Absorption and reduction of methacrolein (MACR) by tomato plants. MACR was vaporized at 560 μL L^{-1} in a glass jar (187 mL) with and without the aerial part of tomato plant (shown in black bars and white bars, respectively). After different incubation periods the concentrations of MACR (A) and isobutyraldehyde (B) in the headspace were examined with HPLC after derivatization to their 2,4-dinitrophenylhydrazones. Bars represent mean ± standard error; $n = 4$. An asterisk in the figure indicates significant difference from the control (two-way ANOVA followed by Tukey, (*), $P < 0.05$; (**), $P < 0.01$).

Figure 2. The amounts of reduced metabolites derived from methacrolein (MACR) in the headspace (A) and in plant tissues (B). The aerial part of tomato plants were exposed to MACR at 560 μl L^{-1} in a closed jar (187 mL), and the amounts of isobutyl alcohol and methallyl alcohol in the headspace and in the plant tissues were determined. These reduced metabolites were undetectable when MACR was vaporized without a plant or a plant was enclosed in the absence of MACR. Bars represent mean ± standard error; $n = 6$ (in panel A) or 3 (in panel B). Different letters indicate significant difference among periods (two-way ANOVA followed by Tukey, $P < 0.05$).

Figure 3. The amount of MACR-GSH (white bars) and MAA-GSH (gray bars) in tomato treated with MACR-vapor. The aerial part of tomato was exposed to 0 (Control: lower panel) or 560 μl L^{-1} (MACR-treated: upper panel) of MACR for 0 to 1440 min in a glass jar (187 mL). Bars represent mean ± standard error; $n = 3$. Different letters indicate significant difference among periods with each compound (two-way ANOVA followed by Tukey, $P < 0.05$).

Figure 4. MACR-GSH to MAA-GSH reduction activity in the presence of NADPH, NADH, or in the absence of any cofactor in tomato shoots treated with MACR-vapor (at 560 μl L^{-1} for 2 h) or air in a 187 mL-glass jar. A crude enzyme extract prepared from exposed tomato leaves was reacted with MACR-GSH for 10 min; thereafter, the amount of MAA-GSH was determined by LC-MS/MS. Bars represent mean ± standard error; n

= 3. An asterisk in the figure indicates significant difference from the control (two-way ANOVA followed by Tukey, (*), $P < 0.05$).

Figure 5. Effect of MACR exposure at 0, 112, 540, or 2240 μL L^{-1} in a glass jar (187 mL) for 2 h on tomato plants. (A) The concentration of MACR left in the headspace of the jar after 2 h in the absence (open circular) and in the presence (filled circular) of a tomato plant. (B) The concentration of isobutyraldehyde formed and emitted from the plant to the headspace. Isobutyraldehyde was not detected in the absence of tomato. (C) The amount of MACR-GSH (open triangles) and MAA-GSH (filled triangles) accumulated in tomato leaves. (D) Amount of total GSH in tomato leaves. (E) *Fv/Fm* values after treatment. For *Fv/Fm* measurement plants in pots were exposed to the given concentration of MACR-vapor in a 3 L glass container. Bars represent mean ± standard error; $n = 4$. Different letters indicate significant difference among MACR concentrations (statistical analysis: (A), two-way ANOVA followed by Tukey, $P < 0.05$; (B to E), one-way ANOVA followed by Tukey, $P < 0.05$) and asterisks in A indicate significant differences between treatments (**, $P < 0.01$).

Figure 6. Metabolism inside cells support the absorption of MACR from the vapor phase. MACR in the vapor phase is distributed into the cell interior at a given equilibrium defined by Henry's law. Because MACR distributed in cells is quickly metabolized into its reduced form and its GSH-adducts, the concentration of MACR in the cells is lowered. Accordingly, more MACR is partitioned into the cell. Conversion rates of MACR exposed at 560 μL L^{-1} for 2 h are shown in parentheses (%, outside/inside). AOR: alkenal/one oxidoreductase, AKR: aldo-keto reductase, GST: glutathione *S*-transferase.

716 **Table I.** Accumulation of MACR-GSH and MAA-GSH in tomato plants exposed to
717 airflow containing MACR.

Concentration of MACR (nL L^{-1})	0	20
	nmol g^{-1} FW	nmol g^{-1} FW
MACR-GSH	0.141 ± 0.04	1.47 ± 0.14**
MAA-GSH	2.13 ± 0.43	37.9 ± 2.84**
Concentration of MACR (nL L^{-1})	0	100
	nmol g^{-1} FW	nmol g^{-1} FW
MACR-GSH	0.147 ± 0.04	6.51 ± 0.87**
MAA-GSH	0.882 ± 0.16	152.5 ± 15.7**

718 Five potted tomato plants were exposed to airflow (at 1.5 L min^{-1}) containing 0, 20, or
719 100 μL L^{-1} MACR for 6 h in a transparent, fluorinated ethylene-propylene copolymer
720 bag (20 to 40 L), then, the amounts of MACR-GSH and MAA-GSH accumulated in
721 tomato leaves were quantified with LC-MS/MS. Mean ± standard error (n = 5) is shown.
722 Asterisks indicate statistically significant difference (t-test, ** $P < 0.01$).
723

Original figure files

Supplemental figure files

Table S1. Parameters used for MRM analysis of GSH conjugates.

	Q1 (Da)	Q3 (Da)	Dwell (msec)	CEP (V)	CE (V)
MACR-GSH	378.133	231.100	200	18.00	19.00
MAA-GSH	380.000	234.000	200	22.35	21.00
Hex-GSH (IS)	392.179	246.100	200	22.82	21.00

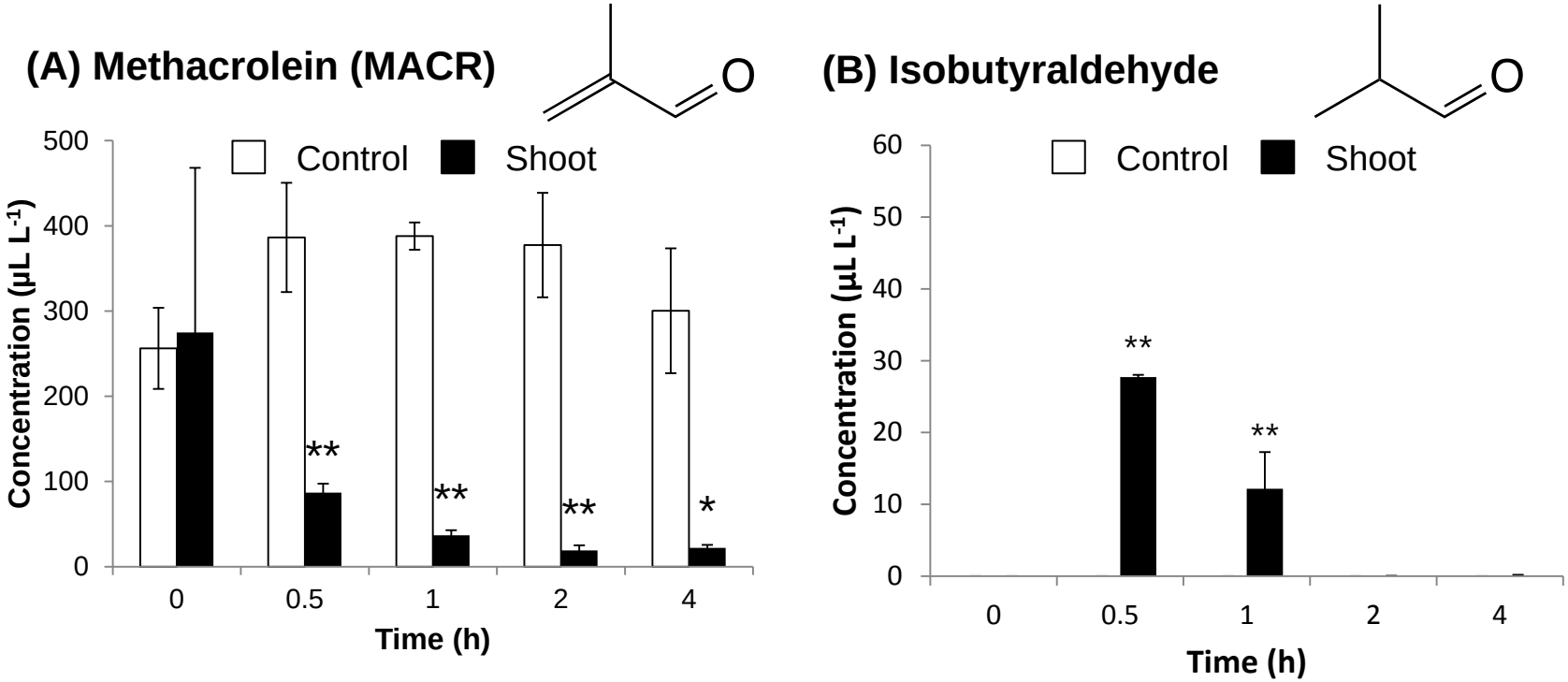

Figure 1. Absorption and reduction of methacrolein (MACR) by tomato plants. MACR was vaporized at 560 µL L^{-1} in a glass jar (187 mL) with and without the aerial part of tomato plant (shown in black bars and white bars, respectively). After different incubation periods the concentrations of MACR (A) and isobutyraldehyde (B) in the headspace were examined with HPLC after derivatization to their 2,4-dinitrophenylhydrazones. Bars represent mean ± standard error; $n = 4$. An asterisk in the figure indicates significant difference from the control (two-way ANOVA followed by Tukey, (*), $P < 0.05$; (**), $P < 0.01$).

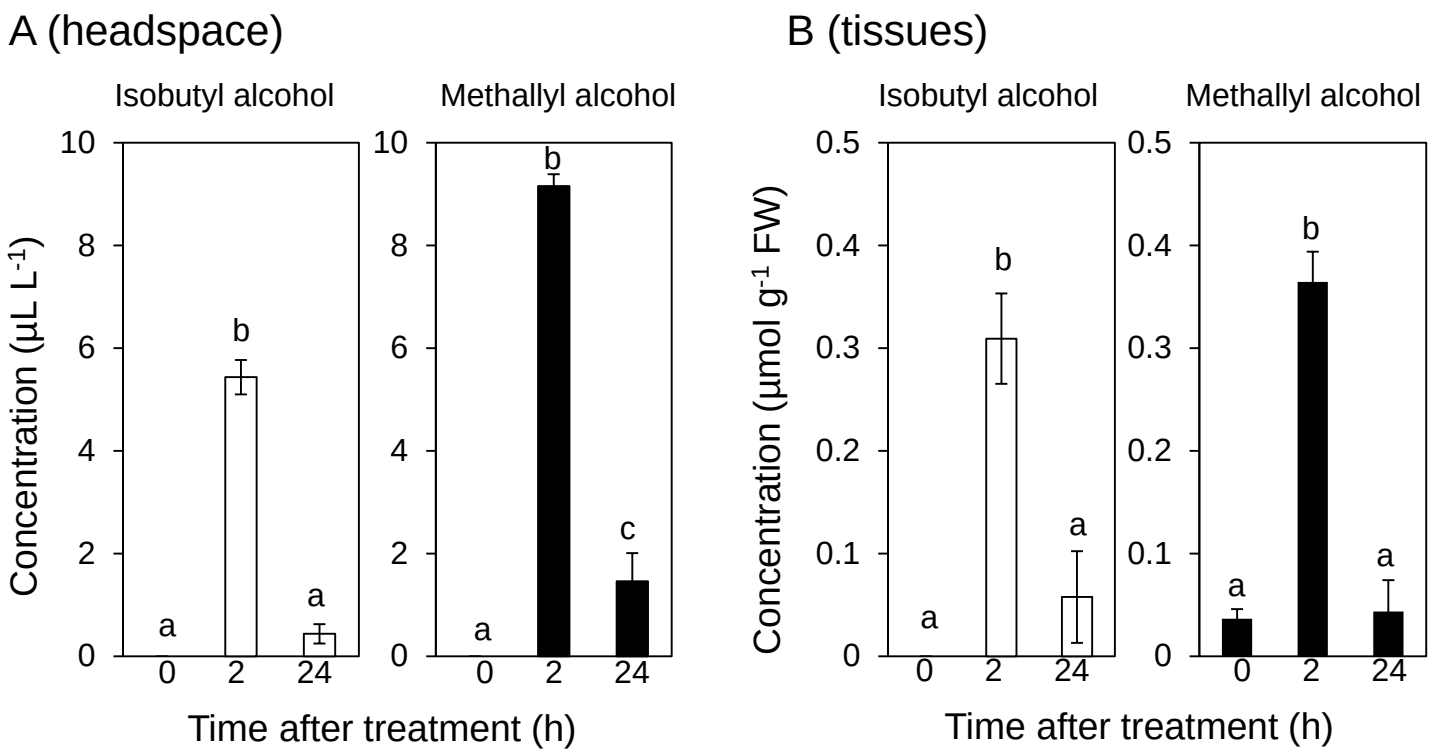

Figure 2. The amounts of reduced metabolites derived from methacrolein (MACR) in the headspace (A) and in plant tissues (B). The aerial part of tomato plants were exposed to MACR at 560 µl L^{-1} in a closed jar (187 mL), and the amounts of isobutyl alcohol and methallyl alcohol in the headspace and in the plant tissues were determined. These reduced metabolites were undetectable when MACR was vaporized without a plant or a plant was enclosed in the absence of MACR. Bars represent mean ± standard error; n = 6 (in panel A) or 3 (in panel B). Different letters indicate significant difference among periods (two-way ANOVA followed by Tukey, $P < 0.05$).

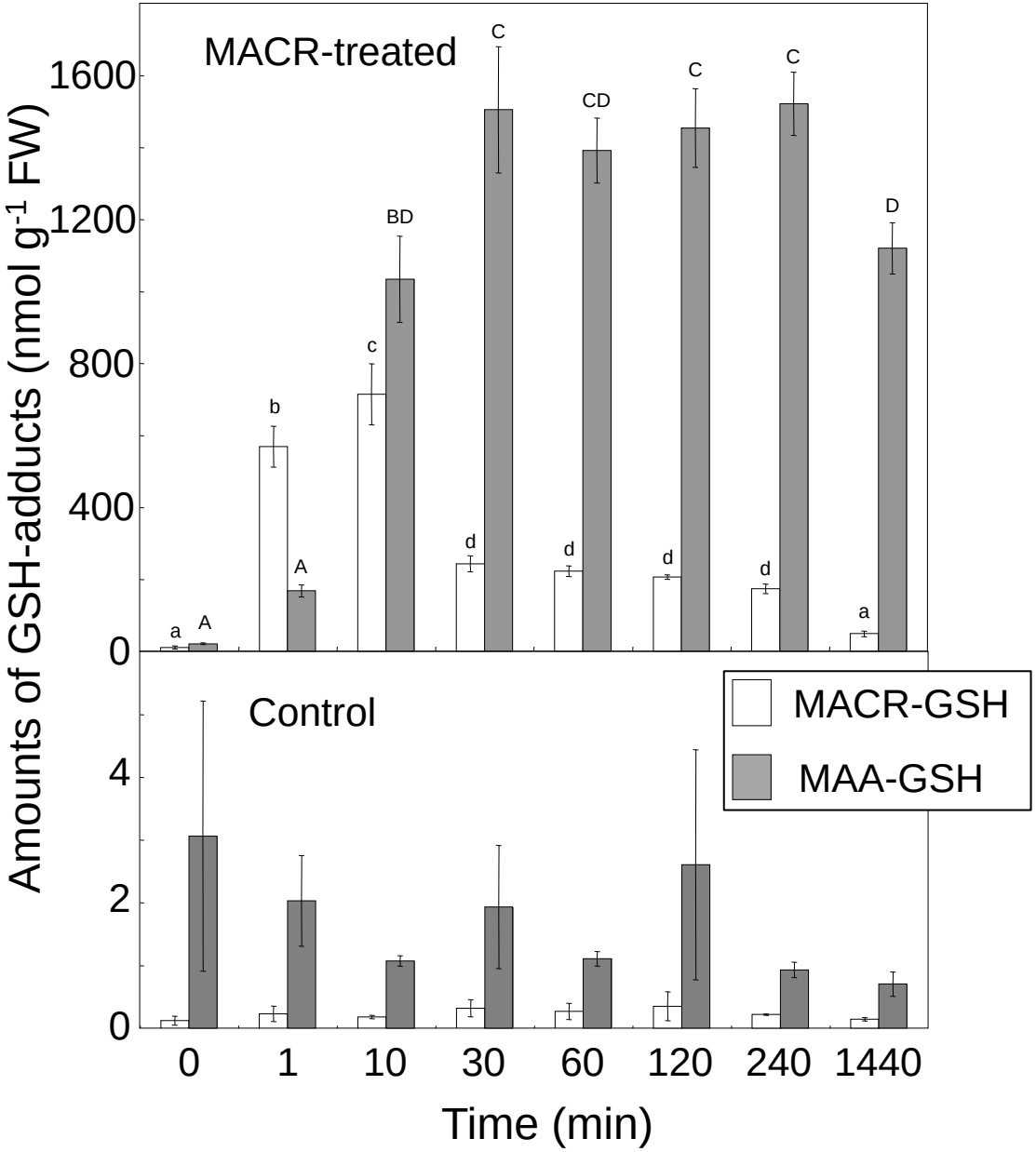

Figure 3. The amount of MACR-GSH (white bars) and MAA-GSH (gray bars) in tomato treated with MACR-vapor. The aerial part of tomato was exposed to 0 (Control: lower panel) or 560 µl L^{-1} (MACR-treated: upper panel) of MACR for 0 to 1440 min in a glass jar (187 mL). Bars represent mean ± standard error, n = 3. Different letters indicate significant difference among periods with each compound (two-way ANOVA followed by Tukey, $P < 0.05$).

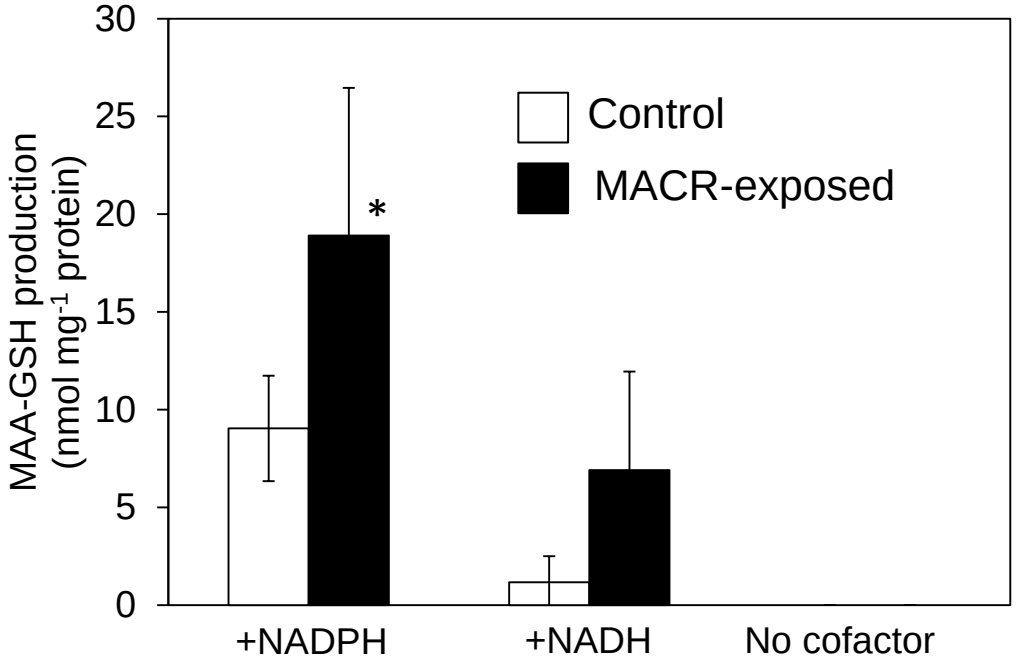

Figure 4. MACR-GSH to MAA-GSH reduction activity in the presence of NADPH, NADH, or in the absence of any cofactor in tomato shoots treated with MACR-vapor (at 560 µl L^{-1} for 2 h) or air in a 187 mL-glass jar. A crude enzyme extract prepared from exposed tomato leaves was reacted with MACR-GSH for 10 min; thereafter, the amount of MAA-GSH was determined by LC-MS/MS. Bars represent mean ± standard error; $n = 3$. An asterisk in the figure indicates significant difference from the control (two-way ANOVA followed by Tukey, (*), $P < 0.05$).

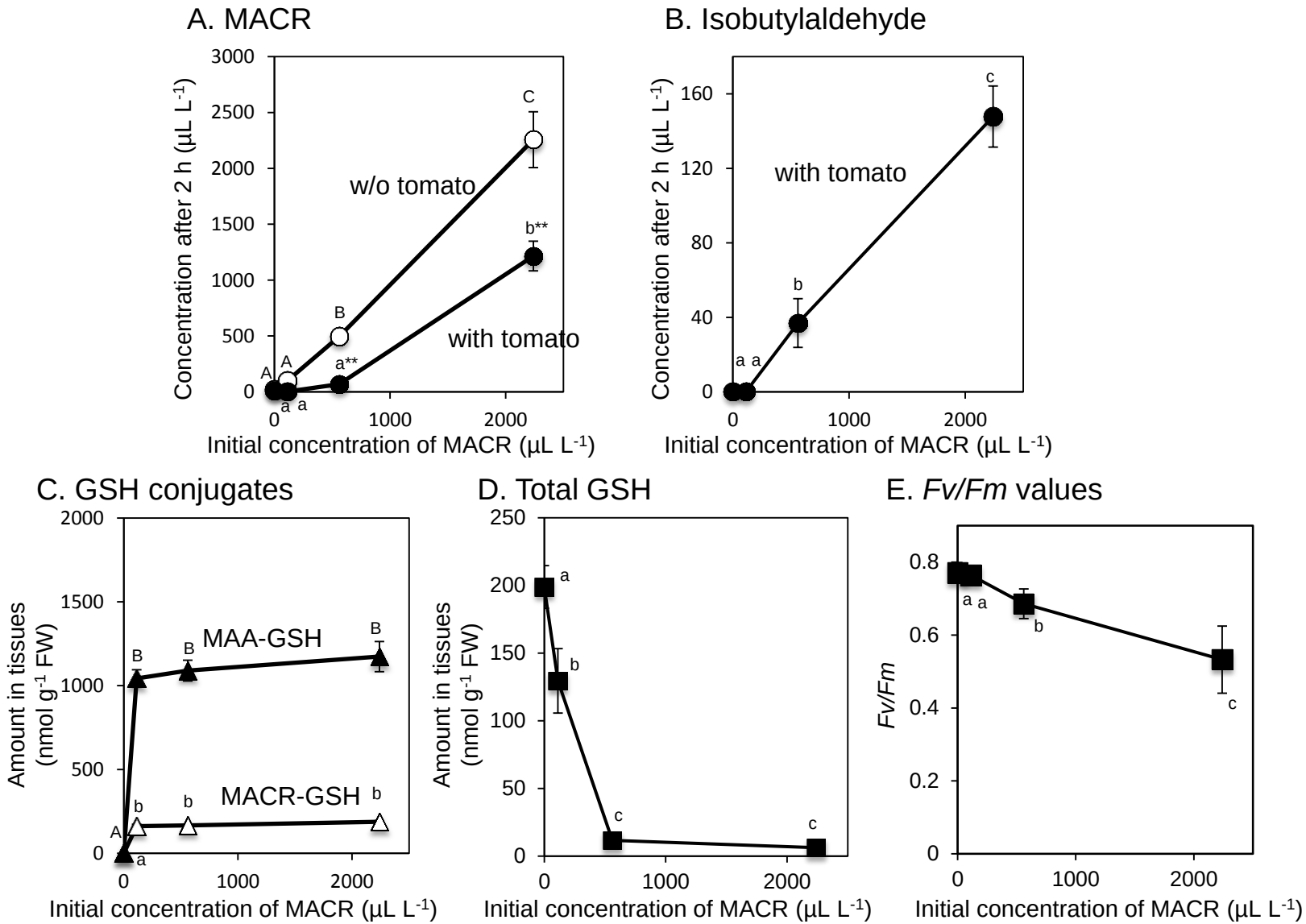

Figure 5. Effect of MACR exposure at 0, 112, 540, or 2240 μL L^{-1} in a glass jar (187 mL) for 2 h on tomato plants. (A) The concentration of MACR left in the headspace of the jar after 2 h in the absence (open circular) and in the presence (filled circular) of a tomato plant. (B) The concentration of isobutyraldehyde formed and emitted from the plant to the headspace. Isobutyraldehyde was not detected in the absence of tomato. (C) The amount of MACR-GSH (open triangles) and MAA-GSH (filled triangles) accumulated in tomato leaves. (D) Amount of total GSH in tomato leaves. (E) *Fv/Fm* values after treatment. For *Fv/Fm* measurement plants in pots were exposed to the given concentration of MACR-vapor in a 3 L glass container. Bars represent mean ± standard error; $n = 4$. Different letters indicate significant differences among MACR concentrations (statistical analysis: (A), two-way ANOVA followed by Tukey, $P < 0.05$; (B to E), one-way ANOVA followed by Tukey, $P < 0.05$) and asterisks in A indicate significant differences between treatments (**, $P < 0.01$).

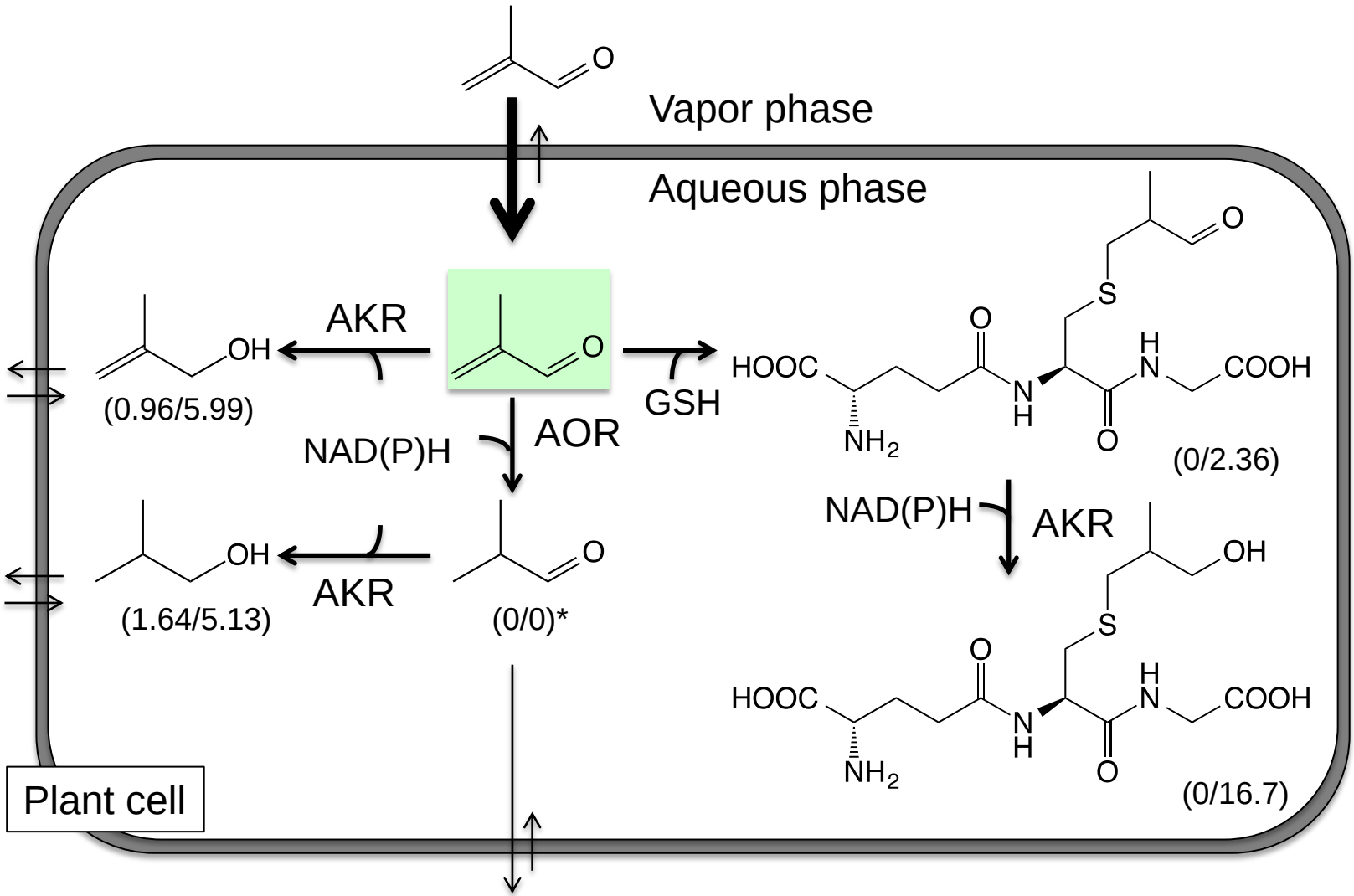

Figure 6. Metabolism inside cells support the absorption of MACR from the vapor phase. MACR in the vapor phase is distributed into the cell interior at a given equilibrium defined by Henry's law. Because MACR distributed in cells is quickly metabolized into its reduced form and its GSH-adducts, the concentration of MACR in the cells is lowered. Accordingly, more MACR is partitioned into the cell. Conversion rates of MACR exposed at 560 $\mu L\ L^{-1}$ for 2 h are shown in parentheses (%, outside/inside). AOR: alkenal/one oxidoreductase, AKR: aldo-keto reductase, GST: glutathione *S*-transferase.

Parsed Citations

Atkinson R, Arey J (2003) Atmospheric degradation of volatile organic compounds. Chem Rev 103: 4605-4638.
Google Scholar: Author Only

Baker NR, Rosenqvist E (2004) Applications of chlorophyll fluorescence can improve crop production strategies: an examination of future possibilities. J Exp Bot 55: 1607-1621.
Google Scholar: Author Only

Böhme A, Thaens D, Schramm F, Paschke A, Shüürmann G (2010) Thiol reactivity and its impact on the ciliate toxicity of ???-unsaturated aldehydes, ketones, and esters. Chem Res Toxicol 23: 1905-1912.
PubMed: http://www.ncbi.nlm.nih.gov/pubmed/20923215?dopt=abstract
Google Scholar: Author Only Title Only Author and Title

Davoine C, Douki T, Iacazio G, Montillet JL, Triantaphylidés C (2005) Conjugation of keto fatty acids to glutathione in plant tissues. Characterization and quantification by HPLC-tandem mass spectropmetry. Anal Chem 77: 7366-7372
Google Scholar: Author Only

Davoine C, Falletti O, Douki T, Iacazio G, Ennar N, Montillet JL, Triantaphylidés C (2006) Adducts of oxylipin electrophiles to glutathione reflect a 13 specificity of the down stream lipoxygenase pathway in the tobacco hypersensitive response. Plant Physiol 140: 1484-1493.
Google Scholar: Author Only

Farmer EE, Mueller MJ (2013) ROS-demiated lipid peroxidation and RES-activated signaling. Ann Rev Plant Biol 64: 429-450
Google Scholar: Author Only

Fedrizzi B, Guella G, Perenzoni D, Gasperotti M, Masuero D, Vrhovsek U, Mattivi F (2012) Identification of intermediates involved in the biosynthetic pathway of 3-mercaptohexan-1-ol conjugates in yellow passion fruit (Passiflora edulis f. flavicarpa). Phytochemistry 77: 287-293.
Google Scholar: Author Only

Goldstein AH, Galbally I (2007) Known and unexplored organic constituents in the Earth's atmosphere. Environ Sci Technol 41: 1514-1521
Google Scholar: Author Only

Griffith QW (1980) Determination of glutathione and glutathione disulfide using glutathione reductase and 2-vinylpyridine. Anal Biochem 106: 207-212.
Google Scholar: Author Only

Guenther A, Hewitt CN, Erickson D, Fall R, Geron C, Graedel T, Harley P, Klinger L, Lerdau M, McKay WA, Pierce T, Scholes B, Steinbrecher R, Tallamraju R, Taylor J, Zimmerman P (1995) A global model of natural volatile organic compound emissions. J Geophys Res 100: 8873-8892.
Google Scholar: Author Only

Guillaume Q, Noctor G (2007) A plate reader method for the measurement of NAD, NADP, glutathione, and ascorbate in tissue extracts: application to redox profiling during Arabidopsis rosette development. Anal Biochem 363: 58-69
PubMed: http://www.ncbi.nlm.nih.gov/pubmed/17288982?dopt=abstract
Google Scholar: Author Only Title Only Author and Title

Iraci LT, Baker BM, Tyndall GS, Orland JJ (1999) Measurements of the Henry's law coefficients of 2-methyl-3-buten-2-ol, methacrolein, and methylvinylk ketone. J Atmos Chem 33: 321-330
Google Scholar: Author Only Title Only Author and Title

Jardine KK, Monson RK, Abrell L, Saleska SR, Srneth A, Jardine A, Ishida FI, Serrano AMY, Arataxo P, Karl T, Fares S, Goldstein A, Loreto F, Huxman T (2012) Within-plant isoprene oxidation confirmed by direct emission of oxidation products methyl vinyl ketone and methacrolein. Global Change Biol 18: 973-984
Google Scholar: Author Only

Jardine KJ, Meyers K, Abrell L, Alves EG, Serrano AMY, Kesselmeier J, Karl T, Guenther A, Chambers JQ, Vickers C (2013) Emission of putative isoprene oxidation products from mango branches under abiotic stress. J Exp Bot 64: 3697-3709
Google Scholar: Author Only

Kalogridis C, Gros V, Sarda-Esteve R, Langford B, Loubet B, Bonsang B, Bonnaire N, Nemitz E, Genard AC, Boissard C, Fernandez C, Ormeño E, Baisnée D, Reiter I, Lathiére J (2014) Concentrations and flux of isoprene and oxygenated VOCs at a French Mediterranean oak forest. Atmos Chem Phys 14: 10085-10102
Google Scholar: Author Only

Karl T, Harley P, Emmons L, Thornton B, Guenther A, Basu C, Turnipseed A, Jardine K (2010) Efficient atmospheric cleansing of oxidized organic trace gases by vegetation. Science 330: 816-819.
Google Scholar: Author Only

Kirch HH, Bartels D, Wei Y, Schnable PS, Wood AJ (2004) The ALDH gene superfamily of Arabidopsis. Trends Plant Sci 9: 371-377.
Google Scholar: Author Only

Kobayashi H, Takase H, Suzuki Y, Tanzawa F, Takata R, Fujita K, Kohno M, Mochizuki M, Suzuki S, Konno T (2011) Environmental stress enhances biosynthesis of flavor precursors, S-3-(hexan-1-ol)-glutathione and S-3-(hexan-1-ol)-L-cysteine, in grapevine through glutathione S-transferase activation. J Exp Bot 62: 1325-1336.
Google Scholar: Author Only

Liu Y, Siekmann F, Renard P, El Zein A, Salque G, El Haddad I, Temime-Roussel B, Voisin D, Thissen R, Monod A (2012) Oligomer and SOA formation through aqueous phase photooxidation of methacrolein and methyl vinyl ketone. Atmos Environ 49: 123-129.
Google Scholar: Author Only

Liu YJ, Herdlinger-Blatt I, McKinney KA, Martin ST (2013) Production of methyl vinyl ketone and methacrolein via the hydroperoxyl pathway of isoprene oxidation. Atmos Chem Phys 13: 5715-5730.
Google Scholar: Author Only

Mano J (2012) Reactive carbonyl species: Their production from lipid peroxides, action in environmental stress, and the detoxification mechanism. Plant Physiol Biochem 59: 90-97.
PubMed: http://www.ncbi.nlm.nih.gov/pubmed/22578669?dopt=abstract
Google Scholar: Author Only Title Only Author and Title

Matsui, K., Sugimoto, K., Kakumyan, P, Khorobrykh, S. A., and Mano, J. (2009) Volatile oxylipins and related compounds formed under stress in plants. Methods Mol. Biol. 580, 17-28.
Google Scholar: Author Only

Matsui K, Sugimoto K, Mano J, Ozawa R, Takabayashi J (2012) Differential metabolisms of green leaf volatiles in injured and intact parts of a wounded leaf meet distinct ecophysiological requirements. PLoS ONE 7: e36433
Google Scholar: Author Only

Meldau DG, Meldau S, Hoang LH, Underberg S, Wünsche H, Baldwin IT (2013) Dimethyl disulfide produced by the naturally associated bacterium Bacillus sp B55 promotes Nicotiana attenuata growth by enhancing sulfur nutrition. Plant Cell 25: 2731-2747.
Google Scholar: Author Only

Mochizuki T, Tani A, Takahashi Y, Saigusa N, Ueyama M (2014) Long-term measurement of terpenoid flux above a Larix kaempferi forest using a relaxed eddy accumulation method. Atmos Environ 83: 53-61.
Google Scholar: Author Only

Omasa K, Tobe K, Hosomi M, Kobayashi M (2000) Absorption of ozone and seven organic pollutants by Populus nigura and Camellia sasanqua. Environ Sci Technol 34: 2498-2500.
Google Scholar: Author Only

Otsuka M, Kenmoku H, Ogawa M, Okada K, Mitsuhashi W, Sassa T, Kamiya Y, Toyomasu T, Yamaguchi S (2004) Emission of ent-kaurene, a diterpenoid hydrocarbon precursor for gibberellins, into the headspace from plants. Plant Cell Physiol 45: 1129-1138.
PubMed: http://www.ncbi.nlm.nih.gov/pubmed/15509835?dopt=abstract
Google Scholar: Author Only Title Only Author and Title

Saito R, Shimakawa G, Nishi A, Iwamoto T, Sakamoto K, Yamamoto H, Amako K, Makino A, Miyake C (2013) Functional analysis of the AKR4C subfamily of Arabidopsis thaliana: model structures, substrate specificity, acrolein toxicity, and responses to light and [CO2]. Biosci Biotechnol Biochem 77: 2038-2045
PubMed: http://www.ncbi.nlm.nih.gov/pubmed/24096666?dopt=abstract
Google Scholar: Author Only Title Only Author and Title

Schöne L, Herrmann H (2014) Kinetic measurements of the reactivity of hydrogen peroxide and ozone towards small atmospherically relevant aldehydes, ketones and organic acids in aqueous solutions. Atmos Chem Phys 14: 4503-4514.
Google Scholar: Author Only Title Only Author and Title

Sugimoto K, Matsui K, Iijima Y, Akakabe Y, Muramoto S, Ozawa R, Uefune M, Sasaki R, Alamgir KM, Akitake S, Nobuke T, Galis I, Aoki K, Shibata D, Takabayashi J (2014) Intake and transformation to a glycoside of (Z)-3-hexenol from infested neighbors reveals a mode of plant odor reception and defense. Proc Natl Acad Sci USA 111: 7144-7149
Google Scholar: Author Only

Tani A, Hewitt CN (2009) Uptake of aldehydes and ketones at typical indoor concentrations by houseplants. Environ Sci Technol 43: 8338-8343.
Google Scholar: Author Only

Tani A, Tobe S, Shimizu S (2013) Leaf uptake of methyl ethyl ketone and croton aldehyde by Castanopsis sieboldii and Viburnum odoratissimum saplings. Atmos Environ 70: 300-306.
Google Scholar: Author Only

Yamauchi Y, Hasegawa A, Taninaka A, Mizutani M, Sugimoto Y (2011) NADPH-dependent reductases involved in the detoxification of reactive carbonyls in plants. J Biol Chem 286: 6999-7009
Google Scholar: Author Only

Yoshida S, Tamaoki M, Ioki M, Ogawa D, Sato Y, Aono M, Kubo A, Saji S, Saji H, Satoh S, Nakajima N (2009) Ethylene and salicylic acid control glutathione biosynthesis in ozone-exposed Arabidopsis thaliana. Physiol Plant 136: 284-298.
Google Scholar: Author Only

Yu GB, Zhang Y, Ahammed GJ, Xia XJ, Mao WH, Shi K, Zhou YH, Yu JQ (2013) Glutathione biosynthesis and regeneration play an important role in the metabolism of chlorothalonil in tomato. Chemosphere 90: 2563-2570
Google Scholar: Author Only

1 **Supplemental figures and table**

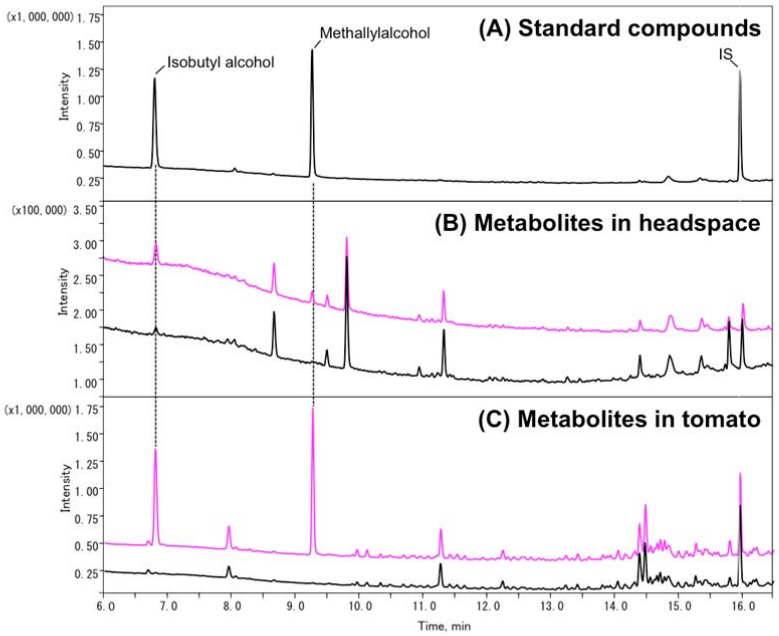

Fig. S1. Total ion chromatogram with GC-MS of reduced metabolites from MACR in the headspace (B) and in tomato tissues (C). (A) Standard compounds. Black chromatogram: extract obtained in the absence of MACR vapor, magenta; extract obtained with MACR-vapor.

2

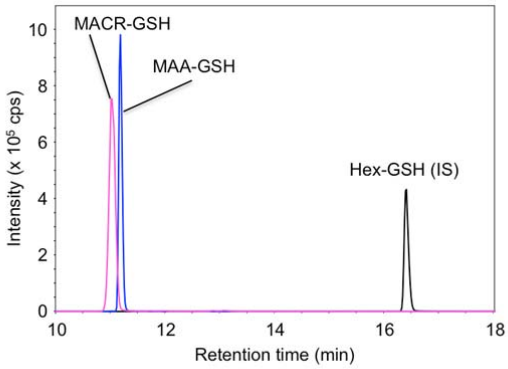

Fig. S2. A representative chromatogram of a mixture of synthetic MACR-GSH, MAA-GSH, and Hex-GSH (included as internal standard) obtained with MRM mode of LC-MS/MS.

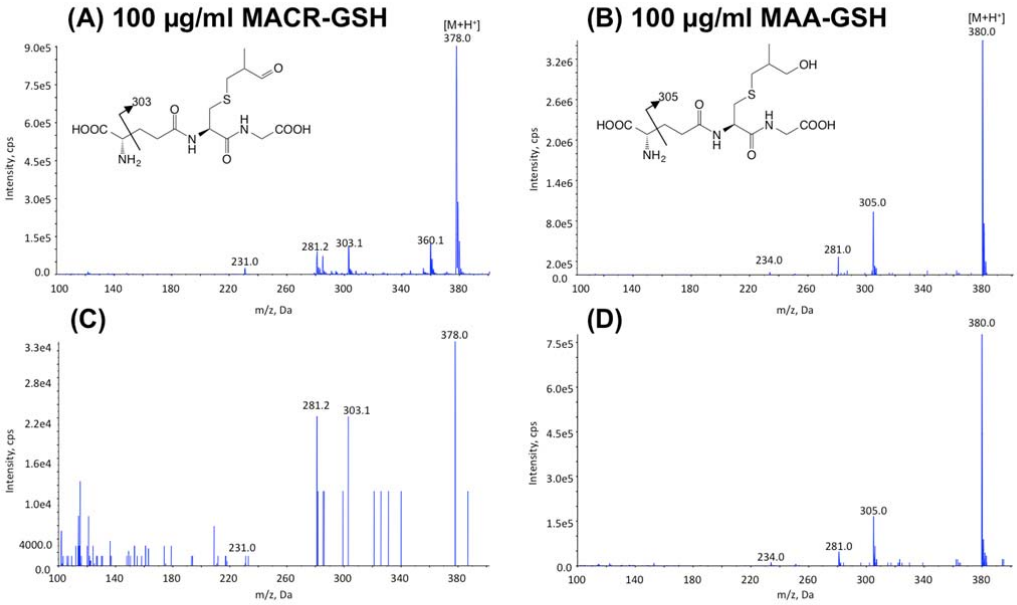

Fig. S3. MS profile of synthesized MACR-GSH (A) and MAA-GSH (B), and the corresponding peaks (C and D) detected in tomato tissues exposed to 560 µL L^{-1} MACR-vapor for 2 h. LC-MS/MS analysis was performed with the enhanced MS mode.

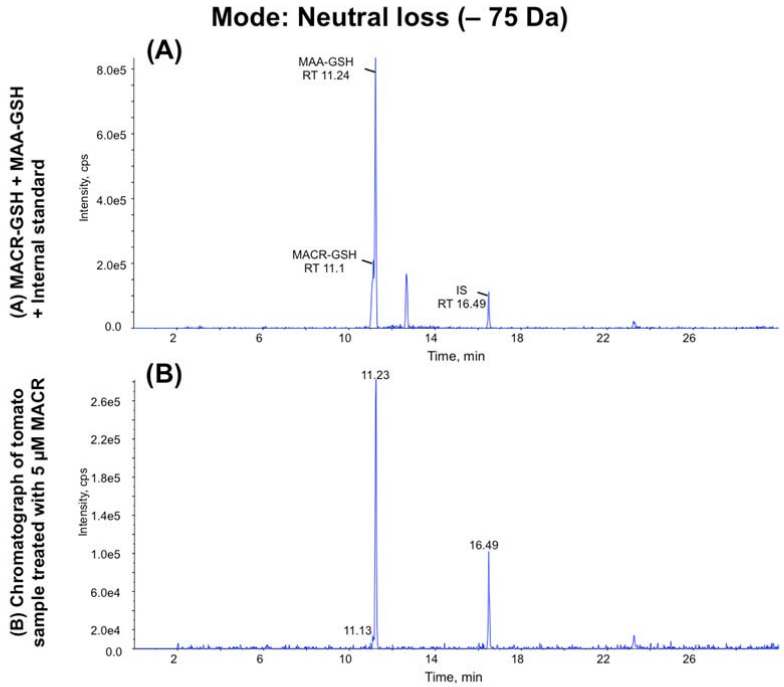

Fig. S4. Chromatogram obtained with the neutral loss mode (-75 Da) of LC-MS/MS to examine GSH conjugates formed in tomato leaves after exposure to MACR. (A) Chromatograph of authentic standards. (B) Chromatograph of extract obtained from tomato sample treated with 560 µL L^{-1} MACR for 2 h.

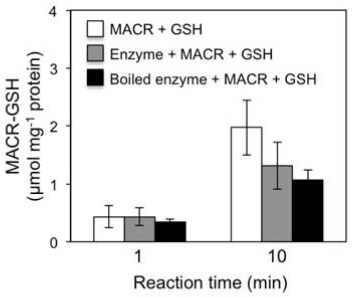

Fig. S5. Effect of addition of crude enzyme solution prepared from tomato leaves on the reaction between GSH and MACR. Reaction was carried out in 0.1 M potassium phosphate, pH 6.5 for 1 and 10 min.

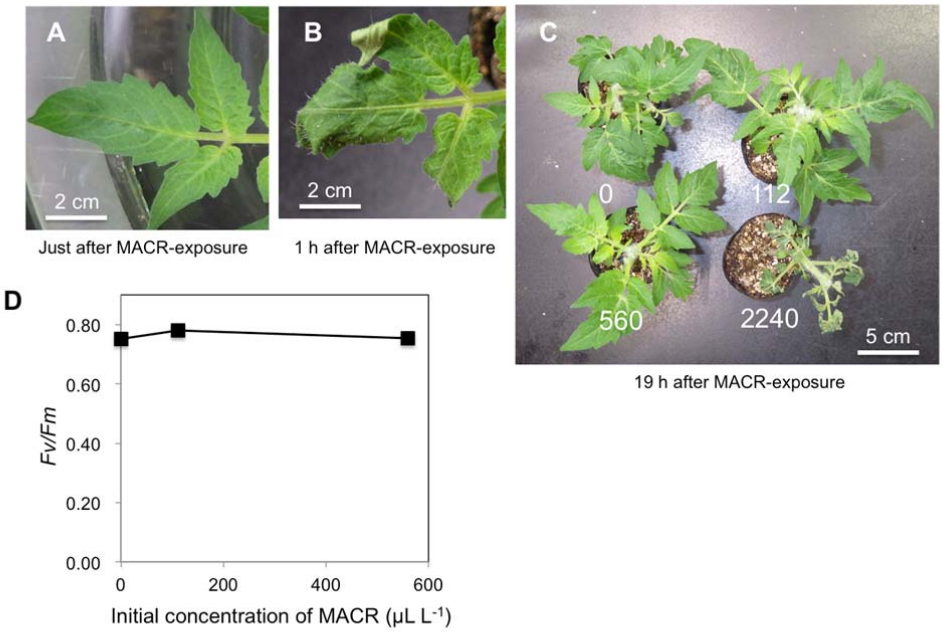

Fig. S6. Consequence of MACR exposure at 0, 112, 540, or 2240 μL L^{-1} for 2 h on tomato plants. After exposing to 2240 μL L^{-1} MACR-vapor for 2 h, the appearance of leaf was examined immediately (A), or after 1 h incubation under light at 25°C without MACR (B). After further incubation of the treated tomato plants under the condition used for growing tomato plants for 19 h without MACR, the plant exposed to 2240 μL L^{-1} withered, but the plants exposed to 0, 112, or 560 μL L^{-1} MACR-vapor looked healthy (C). The *Fv/Fm* ratio examined after the 19 h-incubation showed no significant difference between the plants previously exposed to 0, 112, and 560 μL L^{-1} MACR vapor for 2 h (D, one-way ANOVA followed by Tukey-Kramer).

13 **Table SI.** Parameters used for MRM analysis of GSH conjugates.

	Q1 (Da)	Q3 (Da)	Dwell (msec)	CEP (V)	CE (V)
MAC-GSH	378.133	231.100	200	18.00	19.00
MAA-GSH	380.000	234.000	200	22.35	21.00
Hex-GSH	392.179	246.100	200	22.82	21.00

14

15